A Spectroscopic and Theoretical Investigation of Charge Transfer Complexes between Silver and Nitric Oxide: Infrared Spectra and Density Functional Calculations of $AgNO^{+,0,-}$ and $Ag_x(NO)_y$ Clusters (x, y = 1, 2) in Solid Argon and Neon

Angelo Citra and Lester Andrews*

Department of Chemistry, University of Virginia, Charlottesville, Virginia 22904-4319

Received: October 9, 2000; In Final Form: January 4, 2001

Laser-ablated silver atoms are reacted with nitric oxide, and products are isolated in solid argon and neon. The pseudo-hyponitrite complex $Ag(NO)_2Ag$ is the dominant product, with AgNOAg and AgONNO present in smaller yields. These complexes are shown using density functional theory to include significant charge transfer from silver but are not as ionic as the analogous alkali metal complexes of nitric oxide. The neutral and ionic mononitrosyls $AgNO^+$, AgNO, and $AgNO^-$ are also observed, and qualitative trends in bond lengths and frequencies in this series are discussed.

Introduction

Silver is known to promote the selective catalytic reduction of nitric oxide by light hydrocarbons over alumina.[1−5] Nitric oxide is only weakly bound on Ag(111) at room temperature, but N_2O is formed at 80 K, which involves a $(NO)_2$ surface intermediate.[6] A DFT study of NO on Ag(111) shows that the adsorbed molecule almost completely retains its odd electron and is able to combine with another NO molecule in an adjacent site on the surface to form $(NO)_2$.[7]

In the present work, silver atoms are produced by laser ablation and reacted with nitric oxide, and products are trapped in solid neon and argon. Isolated molecules are characterized by matrix infrared spectroscopy and density functional calculations. Species containing $(NO)_2$ dominate the chemistry, consistent with the behavior of NO on a silver surface described above. The silver complexes AgNOAg, AgONNO, and $Ag(NO)_2Ag$ are observed, as are the mononitrosyl species AgNO, $AgNO^+$, and $AgNO^-$. The bonding in the mononitrosyls is discussed in detail, and the degree of charge transfer in the larger complexes is discussed within the context of the alkali metal complexes $Li^+(NO)^-$, $Li^+(NO)^{2-}Li^+$, and $Li^+(NO)_2{}^{2-}Li^+$.[8−10]

Experimental and Theoretical Methods

The experiment for laser ablation and matrix isolation has been described in detail previously.[11,12] Briefly, the Nd:YAG laser fundamental (1064 nm, 10 Hz repetition rate, 10 ns pulse width, 5−50 mJ/pulse) was focused on a rotating silver metal target. In experiments with neon, a 10% neutral density filter was used to reduce the laser energy. Laser-ablated metal atoms, cations, and electrons were codeposited with nitric oxide at 0.6−0.1% in argon or 1%-0.04% in neon onto a 7−8 K or 4−5 K CsI window at 2−4 mmol/h for 30 min to 2 h. Several isotopic samples ($^{14}N^{16}O$, Matheson; $^{15}N^{16}O$, MDS isotopes, 99%; $^{15}N^{18}O$, Isotec, 99%) and selected mixtures were used. Infrared spectra were recorded at 0.5 cm^{-1} resolution on a Nicolet 750 spectrometer with 0.1 cm^{-1} accuracy using a HgCdTe detector. Matrix samples were annealed at a range of temperatures (20−45 K, argon, and 6−12 K, neon) and subjected to broad-band irradiation by a medium-pressure mercury arc (Philips, 175 W) with the globe removed (λ > 240 nm).

Density functional theory (DFT) calculations were performed on the silver nitrosyls using the Gaussian 94 program.[13] The BPW91 functional was used in all calculations, with the B3LYP functional employed for comparison in selected cases.[14−16] The 6-311+G(d) basis set was used to represent nitrogen and oxygen,[17] and the LanL2DZ ECP basis set was used for silver.[18,19] Such calculations have predicted reliable frequencies for analogous systems,[20] and comparisons of consistent calculations to establish trends are desirable.

Results

Absorptions for silver nitrosyl products in pure and mixed isotopic experiments in solid neon and argon are listed in Tables 1 and 2. Additional bands due to NO, $(NO)_2$, $(NO)_2{}^+$, $(NO)_2{}^-$, NO_2, $NO_2{}^-$, $(NO)_3{}^-$, and N_2O_3 common to experiments with laser-ablated metal and nitric oxide are not listed in the tables.[20−23] The geometries were optimized to standard convergence limits,[13] and associated harmonic frequencies of product molecules calculated using DFT are summarized in Tables 3−6 with calculated charge distributions are given in Tables 7 and 8. Figures 1−4 show spectra in argon and neon matricies in both nitrosyl and nitride-oxide regions, and Figures 5−7 summarize the DFT structures for the larger silver nitrosyl complexes.

Discussion

Product molecules in the silver−nitric oxide reaction are identified by isotopic substitution and DFT calculations as follows.

AgNO. The band observed at 1680.3 cm^{-1} in argon grows during early annealing and irradiation but decreases during the higher temperature annealings. The $^{15}N^{16}O$ and $^{15}N^{18}O$ counterpart bands are observed at 1651.3 and 1606.4 cm^{-1}, giving $^{14}N^{16}O/^{15}N^{16}O$ and $^{15}N^{16}O/^{15}N^{18}O$ isotopic ratios of 1.0176 and 1.0280. No additional bands are observed in either mixed isotopic experiment, which shows that only one NO subunit is involved in the mode. These bands are therefore assigned to AgNO. The ratios are essentially identical to those for isolated nitric oxide (1.0176, 1.0277), which indicates that there is almost no coupling between the Ag−N and N−O stretching modes of

10.1021/jp003706o CCC: $20.00

TABLE 1: Infrared Absorptions (cm^{-1}) Observed for Silver and Nitric Oxide in Neon at 4−5 K

^{14}N^{16}O	^{15}N^{16}O [^{14}N^{16}O/^{15}N^{16} O]	^{15}N^{18}O [^{14}N^{16}O/^{15}N^{16} O]	^{14}N^{16}O + ^{15}N^{16}O	^{15}N^{16}O + ^{15}N^{18}O	assgnt
1912.4	1878.6 [1.0180]	1828.5 [1.0274]	1912.4, *b*	1878.6, *b*	AgNO$^+$ (site)
1910.9	1877.4 [1.0178]	1827.0 [1.0276]	1910.9, *b*	1877.4, *b*	AgNO$^+$
1909.8	1876.1 [1.0180]	1825.7 [1.0276]	1909.8, *b*	1876.1, *b*	AgNO$^+$ (site)
1711.8	1682.4 [1.0175]	1636.8 [1.0279]	1711.8, 1682.4	1682.4, 1636.8	AgNO
1707.3	1678.0 [1.0175]	1632.1 [1.0281]	1707.3, 1678.0	1678.0, 1632.1	AgNO
1479.5	1451.6 [1.0192]	1414.1 [1.0265]	*a*	1451.6, *b*	Ag$_x$(NO)$_y$
1451.5	1426.1 [1.0178]	1388.2 [1.0273]	1451.5, 1427.3	*b*, 1388.9	AgNOAg
1403.7	1379.5 [1.0175]	1341.6 [1.0282]	*b*, 1379.5	*a*	AgNO$^-$ (site)
1399.2	1375.2 [1.0175]	1337.5 [1.0282]	*b*, 1375.l	*a*	AgNO$^-$
1387.5	1358.2 [1.0216]	1330.4 [1.0209]	1387.5, 1382.6, 1364.0, *b*	1358.2, 1355.0, 1333.5, 1330.4	AgONNO
1320.5	1304.4 [1.0123]	1278.3 [1.0204]	1320.5, 1312.2, *b*	1304.4, 1290.5, 1278.3	Ag$_x$(NO)$_2$
1315.8	1300.0 [1.0122]	1274.0 [1.0204]	1315.8, *b*	*a*	Ag$_x$(NO)$_2$ (site)
1309.5	1294.2 [1.0118]	1270.7 [1.0185]	*b*	*a*	Ag$_x$(NO)$_2$ (site)
1193.8	1177.0 [1.0143]	*c*	*b*	*b*	Ag(NO)$_2$Ag
1185.5	1169.3 [1.0139]	1141.5 [1.0244]	1185.8, 1177.2, 1169.6	1169.3, 1154.5, 1141.5	Ag(NO)$_2$Ag
1181.6	1164.6 [1.0146]	1137.3 [1.0240]	*b*	1164.6, 1150.4, 1137.3	Ag(NO)$_2$Ag

[a] Band not observed in this experiment. [b] Spectral region too congested to observe bands. [c] Unresolved bands.

TABLE 2: Infrared Absorptions (cm^{-1}) Observed for Silver and Nitric Oxide in Argon at 7−8 K

^{14}N^{16}O	^{15}N^{16}O [^{14}N^{16}O/^{15}N^{16} O]	^{15}N^{18}O [^{14}N^{16}O/^{15}N^{16} O]	^{14}N^{16}O + ^{15}N^{16}O	^{15}N^{16}O + ^{15}N^{18}O	assgnt
1904.3	*a*	*a*	*a*	*a*	AgNO$^+$
1900.2	*a*	*a*	*a*	*a*	AgNO$^+$ (site)
1680.3	1651.3 [1.0176]	1606.4 [1.0280]	1680.3, 1651.3	1651.3, 1606.4	AgNO
1437.9	1412.3 [1.0181]	1375.1 [1.0271]	1437.9, 1412.3	1412.3, 1375.1	AgNOAg
1431.7	1406.6 [1.0178]	1368.9 [1.0275]	1431.7, 1406.6	1406.6, 1368.9	AgNOAg
1426.6	1401.8 [1.0177]	1364.2 [1.0276]	1426.6, 1401.8	1401.8, 1364.2	AgNOAg
1407.5	1383.5 [1.0174]	1345.4 [1.0283]	1407.5, 1395.0, 1383.5	*a*, 1362.2, 1345.4	Ag$_x$(NO)$_2$
1405.3	1381.5 [1.0172]	1343.4 [1.0284]	1405.3, 1393.2, 1381.5	*a*, 1360.0, 1343.4	Ag$_x$(NO)$_2$
1392.3	1368.2 [1.0176]	1331.1 [1.0279]	1392.3, 1368.2	1368.2, 1331.1	AgNO$^-$
1121.1	1106.1 [1.0136]	1076.0 [1.0280]	1121.1, 1113.0, 1106.1	1106.1, 1092.7, 1076.0	Ag(NO)$_2$Ag
1117.1	1102.1 [1.0136]	*b*	*b*	*b*	Ag(NO)$_2$Ag
1112.8	1097.5 [1.0139]	1071.0 [1.0247]	1112.8, 1105.3, 1097.5s	1097.5, 1084.2, 1071.0	Ag(NO)$_2$Ag
1104.4	1089.3 [1.0140]	1063.2 [1.0246]	1104.4, 1097.0, 1089.3	*b*, 1063.2	Ag(NO)$_2$Ag

[a] Band not observed in this experiment. [b] Spectral region too congested to observe bands.

AgNO. This is unusual since most transition metal mononitrosyls have significantly higher ^{14}N^{16}O/^{15}N^{16}O ratios (∼1.020) and lower ^{15}N^{16}O/^{15}N^{18}O ratios (∼1.022).[24−27]

The analogous band in neon is split into two matrix sites at 1711.8 and 1707.3 cm^{-1} and has the same isotopic ratios. The slightly higher frequency observed in neon is typical for most molecules,[28] but the difference for NO is only 2.6 cm^{-1}.[21,22]

The DFT calculations for AgNO support the above assignment. The ^{1}A′ state has the lowest energy when the BPW91 functional is employed, with an NO stretching frequency of 1671.3 cm^{-1}. This is in excellent agreement with the experimental value in argon, although this functional usually gives frequencies a few tens of wavenumbers too high for transition metal nitrosyl species.[25−27] The ^{1}A″ and ^{3}A″ states are calculated to be only 27 and 14 kJ/mol higher in energy, with frequencies of 1654.9 and 1632.6 cm^{-1}. These are in greater error than that for the ^{1}A′ state, but either could be the correct ground state. The ^{3}A′ state was also calculated but is not bound: the Ag−N separation is 4.391 Å, and the NO stretching frequency of 1892.9 cm^{-1} is almost identical to the frequency 1892.3 cm^{-1} calculated for isolated NO. Similar results are found with the B3LYP functional: the ^{3}A′ state is not bound, and the ^{1}A′, ^{1}A″, and ^{3}A″ states are of similar energy. However, the NO stretching frequency calculated for the ^{3}A″ state is *lower* than the experimental value. Since the B3LYP functional overestimates frequencies, the ^{3}A″ state can be rejected. The frequencies calculated for the ^{1}A′ and ^{1}A″ states are higher than the experimental values and must be scaled down by 0.954 and 0.961 to fit the experimental frequency. These scale factors are typical for this functional and class of molecule,[25−27] and it can be concluded from this that the ground state of AgNO is either ^{1}A′ or ^{1}A″. The Ag−N stretching mode is calculated to be below 400 cm^{-1} in all cases which is below the instrumental limits. The DFT calculations for AgNO described here are completely analogous to those for CuNO. The ^{1}A′ state of CuNO is found to be 12 kJ/mol lower than the ^{3}A″ state with the BP86 functional but 13 kJ/mol higher with the B3LYP functional.[24] However, CCSD(T) calculations for CuNO showed that ^{1}A′ is the correct ground state.[29] Binding energies for the ^{1}A′ states have been estimated by comparing the energy of AgNO (^{1}A′) with that of silver (^{2}S) and NO ($^2\Pi$): the reaction of Ag and NO is clearly exothermic.

The side and oxygen-bound isomers of AgNO have also been explored. No stable side-bound geometry could be found as the structure simply optimized to bent AgNO. Both linear and bent AgON geometries were calculated, and the linear geometries are much higher in energy. The ^{3}A″ state is found to be lowest in energy with both BPW91 and B3LYP and is 49 kJ/mol (BPW91) and 9 kJ/mol (B3LYP) higher in energy than the ^{1}A′ state of AgNO. The optimized geometries for the ^{3}A″ state are very different with each functional; the Ag−O separation is calculated to be 2.669 Å with the BPW91 functional and 3.672 Å with B3LYP. The NO stretching frequencies of 1668.5 and 1957.7 cm^{-1} are consistent with this, the latter being only slightly perturbed from the value of 1980.4 cm^{-1} calculated for isolated NO using B3LYP. The calculated reaction energies show that AgON is probably not bound with either functional, and there is no experimental evidence for this molecule.

AgNO$^-$. A sharp band observed at 1392.3 cm^{-1} in argon decreases in intensity on annealing and irradiation. The ^{15}NO

TABLE 3: Geometries, Energies, and Frequencies Calculated for NO, $(NO)_2$, and Isomers of AgNO Using DFT (BPW91/LanL2DZ/6-311+G(d))

molecule	state (pt group)	rel energies (kJ/mol)	$\langle S^2 \rangle$	geometry (Å, deg)	freq (cm^{-1}) [intensities (km/mol)]
NO	$^2\Pi$ ($C_{\infty v}$)		0.7500	NO: 1.160	1892.3 [39]
trans-$(NO)_2$	^1A_g (C_{2h})			NN: 1.993 NO: 1.164 ∠ONN: 109.0	1846.6 [0], 1728.5 [885], 707.7 0], 247.5 [0], 209.1 [3], 74.1 [0]
AgNO	$^1A'$ (C_s)	0		AgN: 2.263 NO: 1.178 ∠AgNO: 118.9	1671.3 [1289], 361.6 [15], 188.4 [1]
	$^1A''$ (C_s)	+27	0.0315	AgN: 2.279 NO: 1.189 ∠AgNO: 123.0	1654.9 [886], 254.6 [6], 148.6 [2]
	$^3A'$ (C_s)	+52	2.0000	AgN: 4.391 NO: 1.160 ∠AgNO: 149.4	1892.9 [50], 14.1 [0], 36.0 [0]
	$^3A''$ (C_s)	+14	2.0000	AgN: 2.225 NO: 1.193 ∠AgNO: 124.8	1632.6 [954], 281.1 [6], 167.0 [2]
$AgNO^+$	$^2A'$ (C_s)	0	0.7500	AgN: 2.408 NO: 1.137 ∠AgNO: 126.2	1926.1 [632], 253.5 [3], 127.7 [2]
	$^2A^a$ (C_s)	+576	0.7667	AgN: 1.955 NO: 1.247 ∠AgNO: 180.0	1555.6 [0], 500.5 [278], 394.1 [2]
$AgNO^-$	$^2A''$ (C_s)	0	0.7508	AgN: 2.385 NO: 1.223 ∠AgNO: 118.2	1474.2 [1269], 310.8 [13], 140.2 [1]
	$^2A'$ (C_s)	+67	0.7500	AgN: 2.724 NO: 1.193 ∠AgNO: 117.9	1612.3 [1252], 219.5 [1], 64.7 [0]
	$^4A''$ (C_s)	+60	3.7500	AgN: 2.263 NO: 1.244 ∠AgNO: 178.1	1435.2 [684], 190.7 [55], 99.8 [11]
AgON	$^1A'$ (C_s)	+58		AgO: 2.540 ON: 1.174 ∠AgON: 128.7	1653.5 [1250], 273.1 [6], 104.4 [2]
	$^3A''$ (C_s)	+49	2.0000	AgO: 2.669 ON: 1.179 ∠AgON: 131.4	1668.5 [782], 174.5 [1], 70.7 [2]
	$^3\Sigma_g^-$ ($C_{\infty v}$)	+188	2.0000	AgO: 2.080 ON: 1.275 ∠AgON: 180.0	1297.6 [23], 340.9 [28], 142.6 [24]

[a] Symmetry of state unknown due to ambiguous orbital symmetries.

and $^{15}N^{18}O$ counterparts at 1368.2 and 1331.1 cm^{-1} give $^{14}N^{16}O/^{15}N^{16}O$ and $^{15}N^{16}O/^{15}N^{18}O$ isotopic ratios of 1.0176 and 1.0279, respectively. Only the pure isotopic bands are found in either the $^{14}N^{16}O + {}^{15}N^{16}O$ or $^{15}N^{16}O + {}^{15}N^{18}O$ mixed isotopic experiments, indicating that only one NO molecule is involved in the mode. When the experiment is repeated with a trace of CCl_4 (electron trap) in the reagent gas, these bands and $(NO)_2^-$ absorptions are not observed, consistent with assignment to anions.[30-32] The neon counterpart to this band is observed at 1399.2 cm^{-1}, with a weaker site at 1403.7 cm^{-1}. The neon bands display the same irradiation and annealing behavior, and the $^{14}N^{16}O/^{15}N^{16}O$ and $^{15}N^{16}O/^{15}N^{18}O$ isotopic ratios of 1.0175 and 1.0282 are almost identical to those in argon. These observations indicate assignment of the above bands to $AgNO^-$. Mononitrosyl anions have been observed with other transition metals at similar frequencies and sensitivity to annealing and irradiation.[30-32]

The DFT calculations support the assignment to $AgNO^-$. The $^2A''$ state is found to be of lowest energy with the BPW91 functional, with a bond angle of 118.2°. The nitrosyl stretching frequency is calculated to be 1474.2 cm^{-1}, several tens of wavenumbers higher than the observed value. The isotopic ratios are calculated to be 1.0180 and 1.0286, in good agreement with experiment. The same ground state is found with the B3LYP functional, and the calculated frequency of 1492.8 cm^{-1} requires a scale factor of 0.933, similar to that for PdNO and PtNO.[25] Finally, the stretching frequency of 1399.2 cm^{-1} is close to the 1355 cm^{-1} value for NO^- deduced from low-energy electron impact studies,[33] indicating that most of the negative charge is localized on the NO subunit.

$AgNO^+$. A new band is observed at 1904.3 cm^{-1} in argon only when a trace amount of CCl_4 is added to the reagent gas; under these circumstances the $(NO)_2^+$ band is enhanced 1.4-fold and the above anion bands are eliminated. The 1904.3 cm^{-1} band increases on annealing but disappears on irradiation. This behavior is typical of a cation,[30-32] and the 1904.3 cm^{-1} band is assigned to $AgNO^+$. The neon counterpart observed at 1910.9 cm^{-1} increased by a factor of 5 in the $NO/CCl_4/Ne$ experiment relative to AgNO. Isotopic counterparts in the $^{15}N^{16}O$ and $^{15}N^{18}O$ experiments respectively give nitrosyl isotopic frequency ratios of 1.0180 and 1.0274.

The DFT calculations for $AgNO^+$ support this assignment. The BPW91 functional predicts a $^2A'$ ground state, with nitrosyl stretching frequency of 1926.1 cm^{-1}, slightly higher than the observed values in neon and argon. An initially bent $^2A''$ state optimizes to a linear structure 576 kJ/mol higher in energy with incompatible frequencies, and the $^4A'$ and $^4A''$ states are also

TABLE 4: Geometries, Energies, and Frequencies Calculated for $Ag_{1,2}(NO)_{1,2}$ Isomers Using DFT (BPW91/LanL2DZ/6-311+G(d))

molecule	state (pt group)	rel energies (kJ/mol)	$\langle S^2 \rangle$	geometry (Å, deg)	freq (cm^{-1}) [intensities (km/mol)]
AgNOAg	^2A (C_1)	+128	0.7508	AgN: 2.219 NO: 1.200 AgO: 2.509 $\angle$AgNO: 117.6 $\angle$AgON: 126.1 ϕ(AgNOAg):	1488.0 [227], 433.1 [8], 243.7 [9], 186.5 [6], 97.3 [1], 44.1 [2]
	$^4A''$ (C_s)	+146	3.7500	AgN: 2.243 NO: 1.200 AgO: 2.870 $\angle$AgNO: 124.4 $\angle$AgON: 136.3 ϕ(AgNOAg): 180.0	1576.9 [212], 280.1 [8], 172.7 [10], 58.2 [1], 45.8 [2], 16.9 [1]
AgONNO	$^2A''$ (C_s)	0	0.7500	N_1N_2: 1.506 N_1O_1: 1.209 N_2O_2: 1.221 AgN_1: 2.313 AgO_2: 2.596 $\angle N_1N_2O_2$: 109.8 $\angle O_1N_1N_2$: 118.4	1507.2 [547], 1423.7 [421], 810.7 [1], 536.8 [6], ..., 117.8 [1]
$Ag(NO)_2Ag$	^1A_g (C_{2h})	0		N_1N_2: 1.294 N_1O_1: 1.300 Ag_1N_2: 2.422 Ag_1N_1: 2.772 Ag_1O_1: 2.348 $\angle N_1N_2O_2$: 118.4 $\angle O_2Ag_2N_1$: 55.7 ϕ(ONNO): 180.0	1247.6 [0], 1145.9 [396], 1115.5 [0], 732.0 [0], 562.4 [10], ..., 75.1 [0]
	^1B_g (C_{2h})	+55	0.1287	N_1N_2: 1.445 N_1O_1: 1.225 Ag_1N_2: 2.378 Ag_1N_1: 3.120 Ag_1O_1: 2.879 $\angle N_1N_2O_2$: 114.1 $\angle O_2Ag_2N_1$: 49.4 ϕ(ONNO): 180.0	1442.8 [0], 1417.4 [253], 858.4 [0], 545.9 [2], 511.6 [0], ..., 87.3 [0]
	^3B_g (C_{2h})	+55	2.0000	N_1N_2: 1.447 N_1O_1: 1.224 Ag_1N_2: 2.370 Ag_1N_1: 3.119 Ag_1O_1: 2.882 $\angle N_1N_2O$: 114.1 $\angle OAg_2N_1$: 49.4 ϕ(ONNO): 180.0	1444.3 [0], 1416.5 [262], 858.1 [0], 545.2 [2], 506.4 [0], ..., 78.4 [0]

much higher in energy. The $^{14}N^{16}O/^{15}N^{16}O$ and $^{14}N^{16}O/^{15}N^{16}O$ isotopic ratios are calculated to be 1.0180 and 1.0284, in excellent agreement with experiment.

Bonding in AgNO Species. The bonding in the cation, anion, and neutral mononitrosyls has been analyzed using molecular orbitals and natural bond orbitals.[34] The molecular orbitals in $AgNO^+$ are very like those for $CuNO^+$ described previously.[35] The uppermost orbital is bonding between silver and nitrogen and antibonding between nitrogen and oxygen and is predominantly formed from the silver 5s orbital and the in-plane π^* molecular orbital on NO. It is singly occupied in the doublet ground state and gives rise to a one-electron bond between silver and nitric oxide. The next lowest orbitals are composed largely from the 4d orbitals and are highly localized on silver, not contributing to bonding between Ag and NO. This picture is the same for both the BPW91 and B3LYP functionals and accounts for the long Ag−N bond calculated for $AgNO^+$ (2.408 Å, BPW91; 2.431 Å, B3LYP). However, the NBO analyses are different for each functional. With BPW91, a one electron σ type bond between silver and nitrogen is found. This orbital is 15% Ag (97% 5s, 2% 5p, 1% 4d) and 85% N (2% 2s, 98% 2p), very similar to the analogous NBO in $CuNO^+$ (12% Cu and 88% N).[35] The nitrogen and oxygen atoms are bound by a σ bond, an out-of-plane π bond, and a singly occupied in-plane π bond, to a give a bond order of 2.5. The bonding in the NO fragment is described the same way with the B3LYP functional, but no bonding is predicted between silver and nitrogen. The Mulliken and natural charges on silver are less than one (Table 7), which indicates that electron density is transferred from NO to Ag^+. This is consistent with the bonding scheme for $CuNO^+$, which has a one-electron dative bond between the nitrogen and metal, and electron density is transferred to the metal cation. The decreased population of the π^* orbital on NO is reflected in the $AgNO^+$ nitrosyl stretching frequency of 1910.9 cm^{-1} (neon) which is higher than the value of 1874.3 cm^{-1} for NO isolated in neon.

The MO diagram for AgNO is essentially the same as that for $AgNO^+$ except that the Ag−N bonding orbital is now doubly occupied. The composition of the orbital is also different; the contribution from the Ag 5s orbital is increased by ~50%. The greater population of the orbital strengthens the Ag−N bond but weakens the N−O bond, as reflected in the calculated bond lengths and stretching frequencies of AgNO relative to $AgNO^+$. This is also apparent from the NBO analyses which predict a two electron σ bond between silver and nitrogen and a double bond between nitrogen and oxygen, the latter being composed of a σ bond and an out-of-plane π bond. The greater participation by silver in the Ag−N bonding orbital is apparent in the

TABLE 5: Geometries, Energies, and Frequencies Calculated for Isomers of AgNO Using DFT (B3LYP/LanL2DZ/6-311+G(d))

molecule	state (pt group)	rel energies (kJ/mol)	$\langle S^2 \rangle$	geometry (Å, deg)	freq (cm^{-1}) [intensities (km/mol)]
NO	$^2\Pi$ ($C_{\infty v}$)		0.7500	NO: 1.148	1980.4 [46]
trans-$(NO)_2$	^1A_g (C_{2h})			NN: 1.871 NO: 1.155 ∠ONN: 108.6 ϕ(ONNO): 180.0	1900.0 [0], 1773.3 [940], 788.4 [0], 279.0 [0], 267.2 [5], 77.3 [0]
AgNO	$^1A'$ (C_s)	+13		AgN: 2.295 NO: 1.162 ∠AgNO: 117.5	1761.2 [1483], 397.9 [17], 196.1 [2]
	^1A (C_s)	+12	0.0494	AgN: 2.421 NO: 1.170 ∠AgNO: 122.3	1748.6 [1346], 232.9 [7], 113.2 [6]
	$^3A'$ (C_s)	+23	2.0000	AgN: 4.255 NO: 1.148 ∠AgNO: 139.9	1980.9 [55], 36.7 [0], 22.1 [0]
	^3A (C_s)	0	2.0000	AgN: 2.308 NO: 1.179 ∠AgNO: 123.4	1687.9 [1626], 255.9 [11], 143.5 [6]
$AgNO^+$	$^2A'$ (C_s)	0	0.7500	AgN: 2.431 NO: 1.129 ∠AgNO: 127.6	2002.0, [543], 241.4 [2], 135.7 [0]
$AgNO^-$	$^2A''$ (C_s)	0	0.7547	AgN: 2.462 NO: 1.212 ∠AgNO: 118.6	1492.8 [2164], 279.8 [9], 122.2 [0]
	$^4A^a$ (C_s)	+47	3.7501	AgN: 2.293 NO: 1.242 ∠AgNO: 178.8	1490.1 [403], 201.0 [75], 93.9 [7]
AgON	$^1\Sigma^+$ or $^1\Delta$ ($C_{\infty v}$)	+283		AgO: 2.113 ON: 1.237 AgON: 180.0	1389.2 [556], 324.6 [12], 215.3 [34], 129.4 [1]
	$^3\Sigma_g^-$ ($C_{\infty v}$)	+150	2.0000	AgO: 2.078 ON: 1.273 ∠AgON: 180.0	1356.2 [18], 350.8 [40], 157.7 [16]
	$^3A''$ (C_s)	+9	2.0000	AgO: 3.672 ON: 1.149 ∠AgON: 132.3	1957.7 [20], 51.9 [0], 26.3 [0]

[a] Symmetry of state unknown due to ambiguous orbital symmetries.

respective NBO which is 36% Ag (95% 5s, 5% 4d) and 64% N (100% 2p) (BPW91). This bond is therefore best described as a covalent bond formed between the unpaired electrons on Ag and NO which is polarized toward nitrogen. This is illustrated in the charges calculated for AgNO which show a small electron transfer from silver to nitrogen. There is no significant difference between the BPW91 and B3LYP functionals in this case: both give the same bonding description for AgNO.

$AgNO^-$ has a $^2A''$ ground state and the additional electron is in an out-of-plane π^* orbital almost completely localized on NO with a small degree of antibonding π^* character between Ag and N. This weakens the N−O bond and slightly weakens the Ag−N bond with respect to AgNO, as shown by the calculated bond lengths and stretching frequencies. The nitrosyl stretching frequency for $AgNO^-$ is only slightly higher than the experimental value for NO^-, consistent with the addition of an electron to a molecular orbital localized on NO. The next lowest orbital, the HOMO in AgNO, has essentially the same composition as in the neutral molecule, and the 4d orbitals are still highly localized on silver. The NBO analysis for $AgNO^-$ shows a one-electron bond between silver and nitrogen which is 47% Ag (91% 5s, 1% 5p, 8% 4d) and 53% N (2% 2s, 98% 2p) (BPW91) and a double bond between nitrogen and oxygen. The same is found with both functionals and is different to what is expected from the molecular orbital analysis where the singly occupied orbital is only weakly Ag−N antibonding but strongly N−O antibonding. The calculated charges are also surprising; both functionals put the bulk of the negative charge on silver. However this is misleading as the spin densities for $AgNO^-$ show that the unpaired electron is localized on NO. The natural charges, which are considered to be more reliable,[36] also show a greater negative charge on NO. In all the NBO analyses for $AgNO^{+,0,-}$ species, the N−O bonds are found to be ∼40% N and ∼60% O, indicating that these covalent bonds are polarized toward oxygen.

AgNOAg. New bands grow in during annealing at 1437.9, 1431.7, and 1426.6 cm^{-1} in argon, due to the same species in different matrix sites. The $^{15}N^{16}O$ and $^{15}N^{18}O$ counterparts to the 1437.9 cm^{-1} band are 1412.3 and 1375.1 cm^{-1}, giving $^{14}N^{16}O/^{15}N^{16}O$ and $^{15}N^{16}O/^{15}N^{18}O$ isotopic ratios of 1.0181 and 1.0271, respectively. Both the $^{14}N^{16}O + ^{15}N^{16}O$ and $^{15}N^{16}O + ^{15}N^{18}O$ mixed isotopic experiments show only the pure isotope bands, indicating the participation of only one NO subunit. The neon analogue at 1451.5 cm^{-1} is a broad band with identical isotopic ratios.

One possible assignment is to Ag_2NO, the simplest silver nitrosyl cluster species (Figure 5). Molecules of this kind were observed in the platinum and palladium nitrosyl systems, and bands near 1500 cm^{-1} were assigned to Pd_2NO and Pt_2NO where the NO molecule is bound to both metal atoms in a bridged configuration.[25] However, the DFT calculations for bridge-bound Ag_2NO do not support the assignment of this species to the observed bands. The nonplanar $^2A''$ state is found to be lowest in energy using the BPW91 functional, but the calculated NO stretching frequency (1677.0 cm^{-1}) is much higher than the observed bands. A second, asymmetic cluster species AgAgNO has also been calculated, and the ^2A state is

TABLE 6: Geometries, Energies, and Frequencies Calculated for $Ag_{1,2}(NO)_{1,2}$ Isomers Using DFT (B3LYP/LanL2DZ/6-311+G(d))

molecule	state (pt group)	rel energies (kJ/mol)	$\langle S^2 \rangle$	geometry (Å, deg)	freq (cm^{-1}) [intensities (km/mol)]
AgNOAg	^{2}A (C_1)	+134	0.7700	AgN: 2.303 NO: 1.190 AgO: 2.773 AgNO: 119.4 AgON: 130.8 ϕ(AgNOAg): 179.9	1583.0 [294], 305.3 [53], 178.0 [8], 68.1 [2], 51.3 [1], 14.8 [1]
	^{4}A (C_1)	+135	3.7500	AgN: 2.327 NO: 1.182 AgO: 4.003 ∠AgNO: 123.6 ∠AgON: 137.9 ϕ(AgNOAg): 179.9	1654.4 [1256], 280.6 [20], 157.4 [8], 59.3 [1], 17.3 [0], 14.7 [1]
AgONNO	^{2}A (C_1)	0	0.7500	N_1N_2: 1.400 N_1O_1: 1.219 N_2O_2: 1.232 AgN_1: 2.315 AgO_2: 2.533 $\angle N_1N_2O_2$: 110.8 $\angle O_1N_1N_2$: 117.6	1456.3 [481], 1381.9 [385], 897.3 [9], 634.3 [36], 525.8 [19], ..., 122.4 [1]
	^{4}A (C_1)	+103	3.7500	N_1N_2: 1.943 N_1O_1: 1.151 N_2O_2: 1.151 AgN_1: 4.272 AgO_2: 4.226 $\angle N_1N_2O_2$: 114.0 $\angle O_1N_1N_2$: 113.9	
$Ag(NO)_2Ag$	^1A_g (C_{2h})	0		N_1N_2: 1.270 N_1O_1: 1.304 Ag_1N_2: 2.412 Ag_1N_1: 2.760 Ag_1O_1: 2.324 $\angle N_1N_2O_2$: 117.9 $\angle O_2Ag_2N_1$: 55.5 ϕ(ONNO): 180.0	1334.4 [0], 1168.4 [0], 1128.4 [464], 754.8 [0], 574.6 [15], 395.9 [0], ..., 86.8 [22]

TABLE 7: Charges Calculated for $AgNO^{+,0,-}$ Using the BPW91 and B3LYP Functionals

molecule (ground state)	BPW91 Mulliken charges [spin densities] (natural charges)			B3LYP Mulliken charges [spin densities] (natural charges)		
	q_{Ag}	q_N	q_O	q_{Ag}	q_N	q_O
$AgNO^+$ (^{2}A′)	+0.73 [0.20] (+0.82)	−0.06 [0.51] (+0.16)	+0.32 [0.29] (+0.02)	+0.77 [0.15] (+0.87)	−0.03 [0.54] (+0.15)	+0.26 [0.31] (−0.02)
AgNO (^{1}A′)	+0.11 (+0.15)	−0.31 (+0.03)	+0.19 (−0.19)	+0.11 (+0.19)	−0.25 (+0.03)	+0.14 (−0.22)
$AgNO^-$ (^{2}A″)	−0.60 [0.30] (−0.40)	−0.34 [0.90] (−0.19)	−0.06 [0.40] (−0.41)	−0.60 [0.48] (−0.40)	−0.29 [1.03] (−0.17)	−0.11 [0.46] (−0.43)

TABLE 8: Charges Calculated for $Ag_{1,2}(NO)_{1,2}$ Using the BPW91 and B3LYP Functionals

molecule (ground state)	BPW91		B3LYP	
	Mulliken charges [spin densities]	natural charges	Mulliken charges [spin densities]	natural charges
Ag_1NOAg_2 (^{2}A)	q_{Ag_1}: +0.16 [0.04]	+0.21	q_{Ag_1}: +0.14 [0.50]	+0.20
	q_N: −0.34 [0.24]	−0.07	q_N: −0.24 [0.30]	+0.03
	q_O: +0.05 [0.12]	−0.30	q_O: +0.10 [0.17]	−0.25
	q_{Ag_2}: +0.13 [0.68]	+0.16	q_{Ag_2}: 0.0 [0.97]	+0.01
$AgO_2N_2N_1O_1$ (^{2}A″)	q_{Ag}: +0.34 [0.05]	+0.44	q_{Ag}: +0.42 [0.04]	+0.56
	q_{N_1}: −0.31 [0.21]	0.0	q_{N_1}: −0.32 [0.13]	−0.02
	q_{O_1}: −0.05 [0.34]	−0.25	q_{O_1}: −0.09 [0.42]	−0.29
	q_{N_2}: +0.01 [0.20]	+0.11	q_{N_2}: +0.08 [0.14]	+0.12
	q_{O_2}: +0.01 [0.30]	−0.30	q_{O_2}: −0.09 [0.35]	−0.37
$Ag(NO)_2Ag$ (^1A_g)	q_{Ag}: +0.40	+0.56	q_{Ag}: +0.45	+0.63
	q_N: −0.09	−0.02	q_N: −0.10	−0.02
	q_O: −0.31	−0.54	q_O: −0.35	−0.61

found to be 28 kJ/mol lower in energy than Ag_2NO. However, the nitrosyl stretching frequency in this species (1717.8 cm^{-1}) is far too high to account for the observed bands.

Another way to arrange the molecule is to have a silver atom bound on each side of NO but not to each other. This complex is denoted AgNOAg, with one silver bound to nitrogen and the other to oxygen in a trans arrangement. This geometry has been optimized in both doublet and quartet states, and the doublet state is lower in energy by 18 kJ/mol higher. This is within the error of the calculation and either multiplicity could be correct.

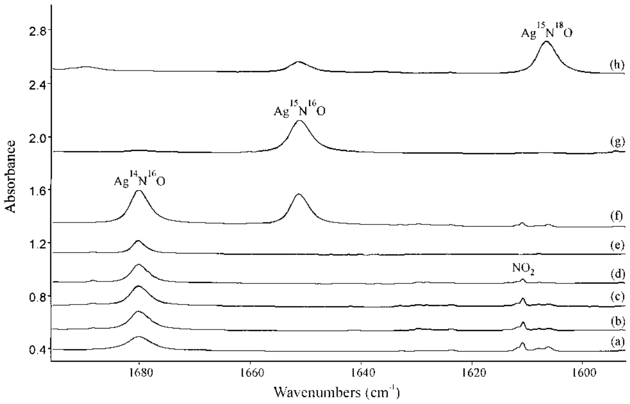

Figure 1. Infrared spectra in the 1700−1590 cm^{-1} region for laser-ablated silver atoms after (a) 60 min of deposition with 0.3% NO in Ar, (b) annealing to 25 K, (c) 25 min of photolysis, (d) annealing to 35 K, (e) annealing to 43 K, (f) 60 min of deposition with 0.15% NO and 0.15% ^{15}NO in Ar and annealing to 25 K, (g) 60 min of deposition with 0.4% ^{15}NO in Ar, and (h) 60 min of deposition with 0.08% ^{15}NO and 0.3% ^{15}N^{18}O in Ar and annealing to 25 K.

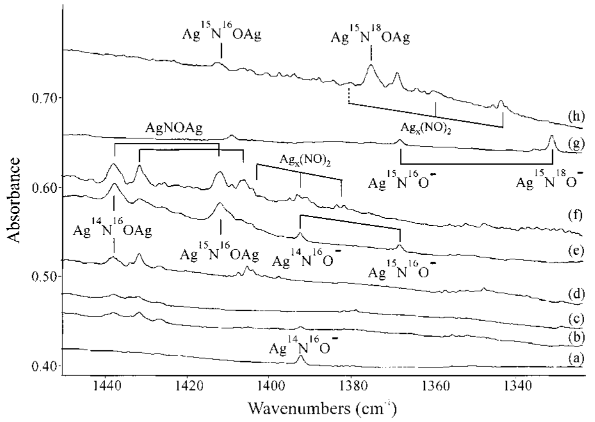

Figure 2. Infrared spectra in the 1450−1320 cm^{-1} region for laser-ablated silver atoms after (a) 60 min of deposition with 0.3% NO in Ar, (b) annealing to 25 K, (c) 25 min of photolysis, (d) annealing to 43 K, (e) 60 min of deposition with 0.15% NO and 0.15% ^{15}NO in Ar and annealing to 25 K, (f) annealing to 43 K, (g) 60 min of deposition with 0.08% ^{15}NO and 0.3% ^{15}N^{18}O, and (h) annealing to 43 K.

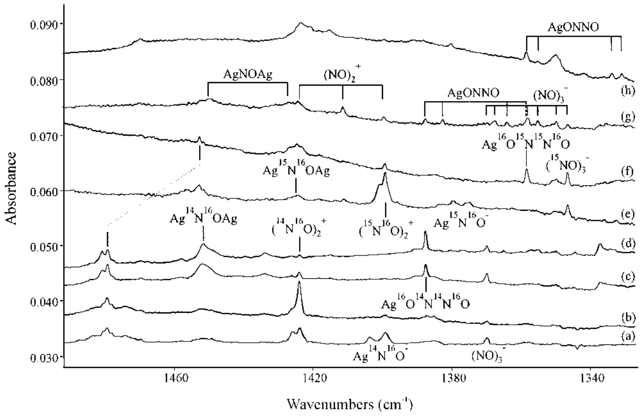

Figure 3. Infrared spectra in the 1500−1330 cm^{-1} region for laser-ablated silver atoms after (a) 50 min of deposition with 0.1% NO in Ne, (b) annealing to 7 K and then 22 min of photolysis, (c) annealing to 10 K, (d) annealing to 12 K, (e) 30 min of deposition with 0.2% ^{15}NO in Ne, (f) annealing to 10 K, (g) 30 min of deposition with 0.15% NO and 0.15% ^{15}NO in Ne and annealing to 10 K, and (h) 60 min of deposition with 0.15% ^{15}NO and 0.15% ^{15}N^{18}O in Ne and annealing to 10 K.

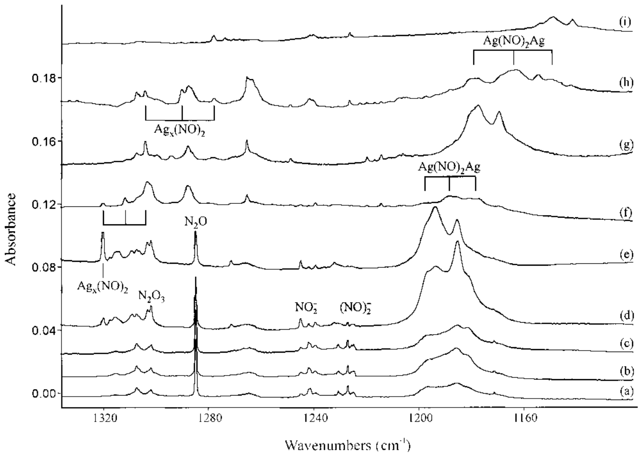

Figure 4. Infrared spectra in the 1330−1120 cm^{-1} region for laser-ablated silver atoms after (a) 50 min of deposition with 0.1% NO in Ne, (b) annealing to 6 K, (c) 22 min of photolysis with 370 nm filter, (d) annealing to 10 K, (e) annealing to 12 K, (f) 30 min of deposition with 0.15% NO and 0.15% ^{15}NO in Ne and annealing to 11 K, (g) 30 min of deposition with 0.2% ^{15}NO in Ne and annealing to 10 K, (h) 60 min of deposition with 0.15% ^{15}NO and 0.15% ^{15}N^{18}O in Ne and annealing to 10 K, and (i) 30 min of deposition with 0.12% ^{15}N^{18}O in Ne and annealing to 12 K.

However, the calculated frequencies provide another means to determine the ground state. The nitrosyl stretching frequency of 1488.5 cm^{-1} calculated for the doublet state is ∼50 cm^{-1} higher than the observed value whereas the analogous frequency for the quartet state is calculated as 1576.9 cm^{-1}, and the latter is therefore rejected. The calculated ^{14}N^{16}O/^{15}N^{16}O and ^{15}N^{16}O/^{15}N^{18}O ratios of 1.0185 and 1.0275 for the doublet state are also in very good agreement with the experimental values of 1.0181 and 1.0271 and support the assignment of these bands to AgNOAg. However, the ^{2}A state of AgNOAg is 114 kJ/mol higher than the ^{2}A″ state of Ag$_2$NO. Similar results are found with the B3LYP functional, where the ^{2}A state of AgNOAg is 126 kJ/mol higher than the ^{2}A″ state of Ag$_2$NO. Even so, the reaction between AgNO and Ag to produce AgNOAg is slightly exothermic, and it is possible that the complex cannot rearrange to a more stable geometry in the low temperature matrix once formed. The band assigned to AgNOAg decreases in intensity by 50% on irradiation, indicating that the complex is rather fragile. This is the most logical assignment, since it is known that only one NO subunit is involved, and the AgNO isomers considered so far cannot explain the observed band. The large difference between the BPW91 and B3LYP geometries for AgNOAg indicates that more sophisticated calculations are required for a good description of the bonding in this species and its energy relative to other structural isomers. The observation of less stable geometric isomers was also found in the platinum nitrosyl system, in which the bridged Pt$_2$NO species was observed in addition to the end bound structure PtPtNO which was calculated to be more stable.[25]

The Mulliken and natural charges for AgNOAg given in Table 8 indicate a substantial charge transfer from the two silver atoms to NO. This explains the low nitrosyl stretching frequency, which approaches that observed for AgNO$^-$ where the extra electron was highly localized on NO, decreasing the bond order through population of the π^* orbitals. This is qualitatively similar to the interaction between alkali metals and nitric oxide in which almost complete charge transfer from the metal occurs, i.e., the NO stretching frequency in the series M$^+$(NO)$^-$ where M = Li−Cs is in the range 1352.5−1374.0 cm^{-1} which is close to the measured frequency of 1355 cm^{-1} for NO$^-$.[8,9,33] Silver is twice as electronegative as lithium, and its complexes with

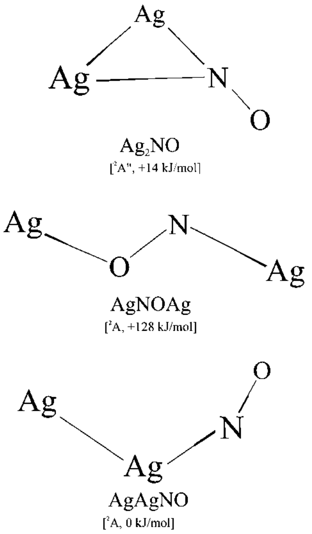

Figure 5. Optimized ground states for isomers of Ag_2NO calculated using the BPW91 functional.

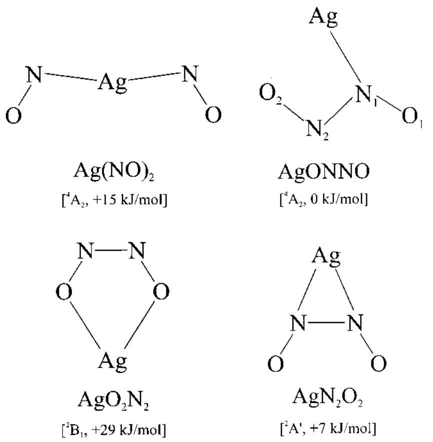

Figure 6. Optimized ground states for isomers of AgN_2O_2 calculated using the BPW91 functional.

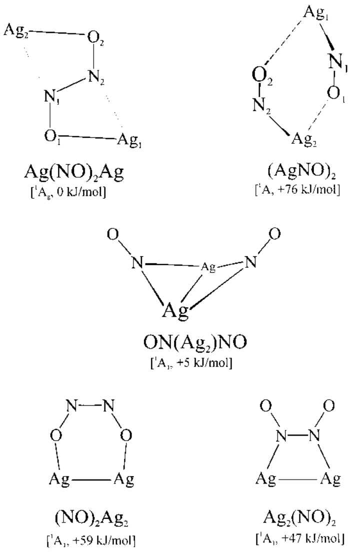

Figure 7. Optimized ground states for isomers of $Ag_2N_2O_2$ calculated using the BPW91 functional.

nitric oxide cannot be described as fully ionic, but the greatly reduced nitrosyl stretching frequency shows that significant charge transfer does occur.

AgONNO. A weak band at 1387.5 cm^{-1} grows in during annealing in neon that is not present initially. The $^{15}N^{16}O$ and $^{15}N^{18}O$ counterparts are observed at 1358.2 and 1330.4 cm^{-1}, to give $^{14}N^{16}O/^{15}N^{16}O$ and $^{15}N^{16}O/^{15}N^{18}O$ isotopic ratios of 1.0216 and 1.0209. These indicate a very large degree of nitrogen motion in the vibrational mode, at the expense of oxygen. Two extra bands are observed at 1382.6 and 1364.0 cm^{-1} in the $^{14}N^{16}O + {}^{15}N^{16}O$ mixed isotope experiment that track with the 1387.5 cm^{-1} band. Four bands are also observed in the $^{15}N^{16}O + {}^{15}N^{18}O$ experiment, the pure isotopic bands at 1358.2 and 1330.4 cm^{-1} and two additional bands at 1355.0 and 1333.5 cm^{-1} that track with these under all conditions. The quartet absorption indicates that two inequivalent NO subunits are involved in the mode and that the observed band is primarily due to one NO group weakly coupled to another NO group. It is likely that this species contains either one or two silver atoms. A dinitrosyl molecule complexed to two silver atoms gives rise to an intense band near 1200 cm^{-1} in neon as described below, and the 1387.5 cm^{-1} band is assigned to a product of formula $Ag(NO)_2$.

Different structural isomers are considered, denoted $Ag(NO)_2$, AgONNO, AgO_2N_2, and AgN_2O_2, as shown in Figure 6. The ground states of each are of comparable energy, but only the frequencies for AgONNO are compatible with the isotopic ratios and mixed isotope splitting patterns observed for the 1387.5 cm^{-1} band, though the bonding is described slightly differently with the BPW91 and B3LYP functionals. The $^4A''$ slate for AgONNO is +94 kJ/mol higher in energy and will not be considered. Two infrared active nitrosyl stretching modes are predicted for AgONNO with the BPW91 functional at 1507.2 and 1423.7 cm^{-1}, with relative intensities of 1.3:1, respectively. The calculated $^{14}N^{16}O/^{15}N^{16}O$ and $^{15}N^{16}O/^{15}N^{18}O$ ratios for the upper band are 1.0193 and 1.0260, significantly larger and smaller than those for AgNO, in qualitative agreement with experiment. The ratios for the lower frequency mode are 1.0189 and 1.0269, in poorer agreement with experiment, and the observed band is therefore assigned to the higher frequency mode of AgONNO. The calculated frequency is 120 cm^{-1} higher than the observed value, and if a similar error is assumed for the other mode, it is expected to be observed near ~1300 cm^{-1}. This region is heavily congested by other absorptions in the 1320−1200 cm^{-1} region and so cannot be observed. The observed mode is mostly due to motion of N_1O_1, with only small involvement of N_2O_2. Correspondingly, the $^{14}N^{16}O + {}^{15}N^{16}O$ mixed isotopic frequencies are predicted at 1506.0 and 1479.9.4 cm^{-1}, very close to the pure isotope bands calculated at 1507.2 and 1478.6 cm^{-1}. This small splitting is again in qualitative agreement with experiment. The B3LYP functional gives similar results but is in better agreement with experiment. The nitrosyl stretching modes are predicted at 1456.3 and 1381.9 cm^{-1}, lower than the BPW91 values. This is unusual, since B3LYP usually overestimates frequencies to a greater extent. The explanation for this is that the B3LYP calculation has more charge transfer from silver, as shown by the calculated charges (Table 8), weakening the N−O bonds and offsetting the usual tendency to give higher frequencies. The optimized geometries are also different; in particular the Ag−O_2 distance is considerably shorter using the B3LYP functional. The $^{14}N^{16}O/^{15}N^{16}O$ and $^{15}N^{16}O/^{15}N^{18}O$ isotopic ratios for the higher frequency band are calculated to be 1.0209 and 1.0233 with B3LYP, and the $^{14}N^{16}O + {}^{15}N^{16}O$ mixed isotopic frequencies are predicted at 1452.4. cm^{-1} and 1431.7 cm^{-1}, a few wavenumbers higher and lower than the calculated pure isotope bands at 1456.3 and 1426.5 cm^{-1}, in agreement with experiment. From this discussion it is clear that B3LYP reproduces the experimental observations more effectively than BPW91, which is only qualitatively correct. Finally, the electron transfer to $(NO)_2$ is not complete, since the observed frequency is considerably higher than the 1227.3 cm^{-1} value for $(NO)_2^-$ in neon.[22]

AgONNO can be viewed as a precursor to $Ag(NO)_2Ag$ described below, in which an additional silver atom is bound to the other side of the $(NO)_2$ subunit. The calculated energies of reaction are very favorable, and most AgONNO combines with silver to form $Ag(NO)_2Ag$, the dominant product in these experiments.

$Ag(NO)_2Ag$. Broad intense bands are observed at 1121.1, 1112.8, and 1104.4 cm^{-1} in argon that are not present initially but grow in strongly during annealing. The former band is the most intense, and the lower frequency bands are due to the same species in different matrix sites. The $^{14}N^{16}O/^{15}N^{16}O$ and $^{15}N^{16}O/^{15}N^{18}O$ ratios for the 1121.1 cm^{-1} band are 1.0136 and 1.0280, respectively, where the former ratio is unusually low. Triplet intensity patterns are observed in both the $^{14}N^{16}O + ^{15}N^{16}O$ and $^{15}N^{16}O + ^{15}N^{18}O$ mixed isotopic experiments; the intermediate bands are observed at 1113.0 and 1092.7 cm^{-1}, indicating that two equivalent NO subunits are involved. Analogous results are found in neon, where three different sites are observed at 1193.8, 1185.5, and 1181.6 cm^{-1} in the $^{14}N^{16}O$ experiment. These bands are far more intense in the 1% NO/Ne experiment and dominate the spectrum, in contrast to the AgNO band at 1711.8 cm^{-1} which is barely visible.

The extremely low nitrosyl stretching frequency and anomalous isotopic ratios for these bands indicate that an unusual nitric oxide product is responsible. A band was observed at 1028.5 cm^{-1} after irradiation in the argon matrix isolation study of lithium, sodium, magnesium, calcium, and barium with nitric oxide.[10] The position of this band is independent of the metal, and it is assigned to the hyponitrite dianion $N_2O_2^{2-}$ isolated in the matrix, where the metal is only an electron source and the metal cation is not bound to the anion. However, the bands present are higher in frequency and unique to the silver system. These product bands are assigned to a pseudo-hyponitrite bound to two silver atoms with incomplete electron-transfer resulting in a complex of $(NO)_2$ rather than isolated $N_2O_2^{2-}$. This is analogous to AgNOAg and AgONNO described above where partial charge transfer to NO occurs, greatly reducing the nitrosyl stretching frequency.

Several geometries with the formula $Ag_2N_2O_2$ have been calculated with DFT and are summarized in Figure 7. The lowest energy structure is found to be $Ag(NO)_2Ag$, which has a silver atom on both sides of *trans*-$(NO)_2$ similar to the structure for $Li(NO)_2Li$.[10] The other structures are all stable, i.e., they have all real frequencies, but the nitrosyl stretching frequencies are far higher than the observed band. Structures with the $(NO)_2$ dimer in a cis arrangement can also be ruled out as two infrared-active nitrosyl stretching modes should be observable, yet no other bands track with the band under consideration. Only the antisymmetric nitrosyl stretching mode of $Ag(NO)_2Ag$ is infrared active: this is calculated to be 1145.9 cm^{-1} for the ^1A_g state (BPW91), in very good agreement with the bands observed in argon. The calculation was repeated with unrestricted orbitals, and orbital occupations were changed to give optimized geometries for the ^1A_u, ^1B_g, and ^1B_u states to see if these were competitive. The ^1B_g state is 55 kJ/mol higher in energy, and the antisymmetric nitrosyl stretching frequency (1417.4 cm^{-1}) is much higher than the observed value. The other states are over 100 kJ/mol higher in energy and are not included in Table 6. The lowest triplet state is 55 kJ/mol higher than the ^1A_g state and has an antisymmetric nitrosyl stretching frequency of 1416.5 cm^{-1}, also considerably higher than experiment. The ^1A_g state is therefore identified as the ground state for $Ag(NO)_2Ag$. The B3LYP calculation for $Ag(NO)_2Ag$ gives the same ground state with an antisymmetric nitrosyl stretching frequency of 1128.4 cm^{-1}. The infrared spectrum of solid $Ag_2N_2O_2$ includes a strong absorption at 1058 cm^{-1} for this mode, which is comparable to the frequency for $Ag(NO)_2Ag$ and suggests that the isolated species described here is similar to the repeating unit within the solid. We find that DFT models the charge-transfer complex $Ag(NO)_2Ag$ quite well but that the extent of charge transfer is sensitive to the functional. This species provides a useful test case for evaluating the effectiveness of different theoretical methods: the observed frequencies and isotopic ratios in neon and argon provide a reference point for comparison. Finally, the calculation for $Ag(NO)_2Ag$ was repeated adding f polarization functions to the LANL2DZ basis set of silver.[36] The optimized geometry is almost identical, and the nitrosyl frequencies are within 5 cm^{-1} of those calculated without the additional f functions.

$Ag_x(NO)_y$. Additional absorptions are observed at 1479.5 and 1320.5 cm^{-1} in neon and at 1407.3 cm^{-1} in argon, and no specific assignments are proposed. No mixed isotopic data is available for the band at 1479.5 cm^{-1}, listed in Table 1 as $Ag_x(NO)_y$. The other bands show triplets in the mixed isotopic experiments and are listed as $Ag_x(NO)_2$.

Surface Studies. The adsorption of NO on silver surfaces has been investigated by several groups.[1−6,37] Adsorbed $(NO)_2$ reacts to form N_2O on warming to 70−90 K. The 1750 cm^{-1} atop frequency for NO on Ag(111) can be compared with our AgNO complex at 1680.3 and 1711.8 cm^{-1} in solid argon and neon, respectively. Although transient species have not been reported, the $Ag_x(NO)_y$ clusters observed here are viable models for transient surface species. In particular AgONNO could decompose to AgO and N_2O.

Conclusions

The reaction of laser-ablated silver atoms with nitric oxide and the subsequent isolation of products in solid neon and argon gives rise to a series of charge-transfer complexes including AgNO, AgNOAg, AgONNO, and $Ag(NO)_2Ag$, as well as the isolated ions $AgNO^+$ and $AgNO^-$. DFT calculations are effective in qualitatively reproducing the experimental observations, but the BPW91 and B3LYP functionals are found to give different results in several cases, indicating that more sophisticated theoretical treatments that include more complete electron correlation effects are required to calculate the electronic structure in these species reliably. These differences are largest in species with interactions between silver and oxygen, the B3LYP functional predicting a stronger bond in AgONNO but a weaker one in AgNOAg, compared to the BPW91 functional. The $Ag_x(NO)_y$ clusters observed here are viable models for transient surface species.

In all cases the degree of charge transfer from silver is found to be less than that in the analogous alkali metal nitrosyl complexes $Li^+(NO)^-$, $Li^+(NO)^{2-}Li^+$, and $Li^+(NO)_2^{2-}Li^+$, which are more ionic. The bonding in $AgNO^+$ is found to be very similar to that in $CuNO^+$: the metal cation is bound to NO via a one-electron dative bond from the nitrosyl fragment. Similar analyses for AgNO and $AgNO^-$ qualitatively account for the calculated bond lengths and nitrosyl stretching frequencies in these species which range from 1910.9 to 1711.8 to 1399.2 cm^{-1} in solid neon for $AgNO^+$, AgNO, and $AgNO^-$, respectively.

Acknowledgment. We gratefully acknowledge financial support from NSF Grant CHE 00-78836.

References and Notes

(1) Miyadera, T. *Appl. Catal., B* **1993**, *199*, 2.

(2) Tatsuo, M.; Yoshida, K. *Chem. Lett*. **1993**, 1483.

(3) Masuda, K.; Tsujimura, K.; Shinoda, K.; Kato, T. *Appl. Catal., B.* **1996**, *33*, 8.

(4) Sumiya, S.; He, H.; Akira, A.; Takezawa, N.; Yoshida, K. *J. Chem. Soc., Faraday Trans.* **1998**, *94*, 2217.

(5) Meunier, F. C.; Breen, J. P.; Zuzaniuk, V.; Olsson, M.; Ross, J. R. H. *J. Catal.* **1999**, *187*, 493.

(6) Brown, W. A.; King, D. A. *J. Phys. Chem. B* **2000**, *104*, 2579 and references therein.

(7) Perez-Jigato, M.; King, D. A.; Yoshimori, A. *Chem. Phys. Lett.* **1999**, *300*, 639.

(8) Milligan, D. E.; Jacox, M. E. *J. Chem. Phys.* **1971**, *55*, 3404.

(9) Tevault, D. E.; Andrews, L. *J. Phys. Chem* **1973**, *77*, 1640.

(10) Andrews, L.; Liang, B. *J. Am. Chem. Soc.*, in press.

(11) Burkholder, T. R.; Andrews, L. *J. Chem. Phys.* **1991**, *95*, 8697.

(12) Hassanzadeh, P.; Andrews, L. *J. Phys. Chem. A* **1992**, *96*, 9177.

(13) Frisch, M. J.; Trucks, G. W.; Schlegel, H. B.; Gill, P. M. W.; Johnson, B. G.; Robb, M. A.; Cheeseman, J. R.; Keith, T.; Petersson, G. A.; Montgomery, J. A.; Raghavachari, K.; Al-Laham, M. A.; Zakrzewski, V. G.; Ortiz, J. V.; Foresman, J. B.; Cioslowski, J.; Stefanov, B. B.; Nanayakkara, A.; Challacombe, M.; Peng, C. Y.; Ayala, P. Y.; Chen, W.; Wong, M. W.; Andres, J. L.; Replogle, E. S.; Gomperts, R.; Martin, R. L.; Fox, D. J.; Binkley, J. S.; Defrees, D. J.; Baker, J.; Stewart, J. P.; Head-Gordon, M.; Gonzalez, C.; Pople, J. A. *Gaussian 94, Revision B.1*; Gaussian, Inc.: Pittsburgh, PA, 1995.

(14) Becke, A. D. *Phys. Rev. A* **1988**, *38*, 3098.

(15) Perdew, J. P.; Wang, Y. *Phys. Rev. B* **1992**, *45*, 13244.

(16) Becke, A. D. *J. Chem. Phys.* **1993**, *98*, 5648.

(17) Krishnan, R.; Binkley, J. S.; Seeger, R.; Pople, J. A. *J. Chem. Phys.* **1980**, *72*, 650.

(18) Wadt, W. R.; Hay, P. J. *J. Chem. Phys.* **1985**, *82*, 284.

(19) Hay, P. J.; Wadt, W. R. *J. Chem. Phys.* **1985**, *82*, 299.

(20) Zhou, M.; Andrews, L. *J. Phys. Chem. A* **2000**, *104*, 3915 (Ni + NO) and references therein.

(21) Andrews, L.; Zhou, M.; Willson, S. P.; Kushto, G. P.; Snis, A.; Panas, I. *J. Chem. Phys.* **1998**, *109*, 177 (argon) and references therein.

(22) Andrews, L.; Zhou, M. F. *J. Chem. Phys.* **1999**, *111*, 6036 (neon) and references therein.

(23) Lugez, C. L.; Thompson, W. E.; Jacox, M. E.; Snis, A.; Panis, I. *J. Chem. Phys.* **1999**, *110*, 10345.

(24) Zhou, M.; Andrews, L. *J. Phys. Chem. A* **2000**, *104*, 2618 (Cu + NO).

(25) Citra, A.; Andrews, L. *J. Phys. Chem. A* **2000**, *104*, 8160 (Pd, Pt + NO).

(26) Citra, A.; Andrews, L. *J. Phys. Chem. A* **2000**, *104*, 11897 (Rh, Ir + NO).

(27) Citra, A.; Andrews, L. *J. Phys. Chem. A* **2000**, *104*, 8689 (Os, Ru + NO).

(28) Jacox, M. E. *Chem. Phys.* **1994**, *189*, 149.

(29) Hrusak, J.; Koch, W.; Schwarz, H. *J. Chem. Phys.* **1994**, *101*, 3898.

(30) Zhou, M. F.; Andrews, L. *J. Phys. Chem. A* **1999**, *103*, 7773 (Rh + CO).

(31) Zhou, M. F.; Andrews, L. *J. Chem. Phys.* **1999**, *110*, 10370 (Fe + CO); **1999**, *111*, 4548 (Cu + CO).

(32) Liang, B.; Zhou, M. F.; Andrews, L. *J. Phys. Chem. A* **2000**, *104*, 3905 (Pd, Pt + CO).

(33) Spence, D.; Schulz, G. J. *Phys. Rev. A* **1968**, *3*, 1971.

(34) Reed, A. E.; Curtiss, L. A.; Weinhold, F. *Chem. Rev.* **1988**, *88*, 899.

(35) Thomas, J. L. C.; Bauschlicher, C. W., Jr.; Hall, M. B. *J. Phys. Chem. A* **1997**, *101*, 8530.

(36) Ehlers, A. W.; Bohme, M.; Dapprich, S.; Gobbi, A.; Hollwarth, A.; Jonas, V.; Kohler, K. F.; Stegmann, R.; Veldkamp, A.; Frenking, G. *Chem. Phys. Lett.* **1993**, *208*, 111.

(37) So, S. K.; Franchy, R.; Ho, W. *J. Chem. Phys.* **1989**, *91*, 5701; **1991**, *95*, 1385.